

Timing Constraints of Gold Mineralization along the Carlin Trend Utilizing Apatite Fission-Track, $^{40}\text{Ar}/^{39}\text{Ar}$, and Apatite (U-Th)/He Methods

A. M. CHAKURIAN,¹ G. B. AREHART,[†]

Department of Geological Sciences, University of Nevada, Reno, Mail Stop 172, Reno, Nevada 89557

R. A. DONELICK,

Department of Geology and Geological Engineering, University of Idaho, Moscow, Idaho 83844

X. ZHANG,

Department of Geological Sciences, Ohio State University, Columbus, Ohio 43210

AND P. W. REINERS²

Department of Geology, Washington State University, Pullman, Washington 99164

Abstract

Apatite fission-track analysis is used to demonstrate that the timing of gold mineralization at the Carlin East and Betze-Post deposits is 37.3 ± 1.5 Ma, based on the weighted mean of measured fission-track ages, and 41.6 ± 1.6 Ma, based on the weighted mean of the ages of the oldest fission tracks retained. Regional measured apatite fission-track ages cluster between 28 and 41 Ma to the south of the Carlin East deposit whereas measured ages are greater than ~56 Ma to the north. The regional trend of the apatite fission-track ages and the pattern of gravity and magnetic anomalies suggest that the thermal center for gold mineralization along the Carlin trend was south of the Carlin East deposit, near the 37 Ma Welches Canyon stock. Modeling of apatite fission-track-age data on both sides of the Post fault indicates that the Little Boulder stock was approximately 35°C cooler at 40 Ma relative to similarly positioned samples in the Goldstrike stock. It is unclear whether this thermal history difference across the Post fault is due to post-40 Ma differential exhumation or differential heating across the fault at the time of gold mineralization. Comparison of apatite fission-track and whole-rock $^{40}\text{Ar}/^{39}\text{Ar}$ ages from altered dikes in the ore zone at Carlin East demonstrates that $^{40}\text{Ar}/^{39}\text{Ar}$ ages do not reflect the age of gold mineralization, whereas the apatite fission-track ages were completely reset at the time of hydrothermal activity. (U-Th)/He ages are younger than the inferred mineralization age and may reflect weak hydrothermal activity associated with Miocene volcanism.

Introduction

CARLIN-TYPE disseminated gold deposits are among the most important types of gold systems in the world because of their large resources and relatively low cost of production. The Carlin deposit (type locality) is located in northeast Nevada, 40 km northwest of the town of Elko (Fig. 1). The Carlin trend in northeastern Nevada hosts several important individual deposits and, as of 1997, in excess of 100 Moz of gold had been identified along this trend (Teal and Jackson, 1997).

The geology of Carlin-type gold deposits has been summarized by Radtke (1985), Arehart (1996), and Hofstra and Cline (2000). Carlin-type gold deposits comprise large disseminated deposits with the Au hosted as submicron inclusions or lattice constituents in hydrothermal pyrite and quartz. Gold is present primarily as a lattice constituent of arsenian pyrite. Associated with the deposition of Au are anomalous As, Sb, Hg, Tl, and Ba. Gold deposition has been observed to be strongly controlled either lithologically, structurally, or both. Host rocks for the deposits are predominantly silty carbonates to calcareous siltstones, although other rock types may host ore locally. Three major types of hydrothermal alteration have been recognized in Carlin-type deposits: decarbonatization, silicification or

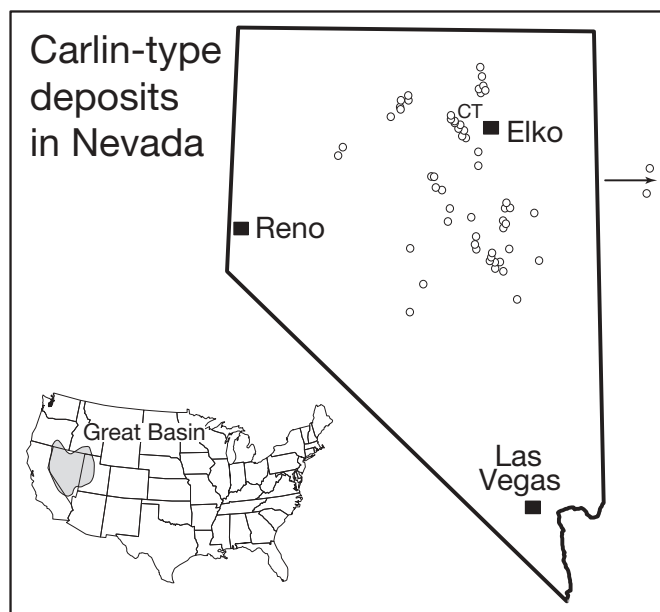


FIG. 1. Location map of Carlin-type deposits in Nevada. CT = Carlin trend.

[†] Corresponding author: e-mail, arehart@unr.edu

jasperoid formation, and argillization (generally distal to proximal, respectively). The relative paragenetic position of these events and their relation to gold ore may vary between deposits, or within a single deposit, probably reflecting fluctuations in each hydrothermal system through time, or multiple episodes of mineralization. Fluid inclusion data suggest that Carlin-type ore fluids were near 225°C and that the depth of formation of the systems was between 2 and 4 km assuming lithostatic pressure.

Along the Carlin trend, Carlin-type deposits are hosted primarily in rocks of Silurian to Devonian age belonging to the Roberts Mountains and Popovich Formations (Evans, 1980; Teal and Jackson, 1997). There have been numerous igneous-hydrothermal events in the area, beginning with emplacement of Jurassic stocks and dikes (ca. 158–150 Ma; Arehart et al., 1993b) and their associated weak skarn mineralization (primarily W-Zn-As). Cretaceous igneous events are represented by the Richmond stock (106 Ma; Evans, 1980) and Cu-Au porphyry mineralization near Gold Quarry (Teal and Jackson, 1997). Dikes and temporally associated Carlin-type alteration and mineralization reflect Eocene events, and weak hot-spring-type and epithermal low-sulfidation veins of probable Miocene age are present in the northern Carlin trend (Ressel et al., 2000a, b).

The timing of gold mineralization in many Carlin-type deposits has not been well constrained. Only one radioisotopic dating technique, Rb/Sr dating of the mineral galkhaite, has been shown to document the timing of gold mineralization of a Carlin-type deposit directly (~39 Ma for the Getchell deposit: Tretbar et al., 2000; ~40 Ma for the Rodeo deposit: Arehart et al., 2003). Understanding of the timing of gold mineralization of Carlin-type gold deposits in the Great basin is critical to the development of genetic models for the formation of these important deposits.

This paper presents results of an apatite fission-track study of the northern Carlin trend, along with a comparison of $^{40}\text{Ar}/^{39}\text{Ar}$ analyses of five altered dikes and two apatite (U-Th)/He ages. Our goals were (1) to determine whether apatite fission-track ages reflect the timing of Carlin-type gold mineralization, (2) to develop a regional paleothermal picture of the northern Carlin trend, (3) to compare the results of apatite fission-track ages with results obtained by $^{40}\text{Ar}/^{39}\text{Ar}$ and (U-Th)/He dating techniques on altered and mineralized igneous rocks, and (4) to examine the uplift history of the Post fault, a major fluid conduit for mineralizing fluids. Each of these aspects of the study contributes to both exploration and genetic models for this important type of gold deposit.

Sample Collection and Analytical Techniques

Three dating techniques were used during the present study: fission-track dating of apatite, $^{40}\text{Ar}/^{39}\text{Ar}$ dating of sericite-altered lamprophyre dikes, and (U-Th)/He dating of apatite. Samples analyzed by the $^{40}\text{Ar}/^{39}\text{Ar}$ technique were collected only from the Carlin East deposit. The samples for apatite fission-track and (U-Th)/He analyses were collected both from the Carlin East deposit (Fig. 2) and more regionally along the northern Carlin trend.

Sample collection and mineral separation

In the Carlin East deposit proper, apatite fission-track samples were collected from both Paleozoic sedimentary rocks

and Jurassic lamprophyre dikes exposed in underground workings and in the pit in an attempt to determine if there is a deposit-wide age or thermal zonation pattern. Samples for $^{40}\text{Ar}/^{39}\text{Ar}$ dating (Figs. 3 and 4) were obtained from argillized and sericitized lamprophyre dikes containing greater than 0.5 ppm Au to see if the gold-bearing hydrothermal fluids had partially or fully reset the sericite grains or if new (gold age) sericite was present. Lamprophyre dikes are considered to be slightly younger than the Goldstrike stock and, where similar dikes have been dated in the Carlin trend, yield crystallization ages of ca. 150 Ma. At two locations, samples were collected for both apatite fission-track and $^{40}\text{Ar}/^{39}\text{Ar}$ dating for comparison of the two techniques.

Samples collected regionally along the Carlin trend were obtained primarily for the purpose of examining zonation of apatite fission-track ages at the district scale. These samples were collected along a north-south traverse that extends from the Richmond stock in the south to the Goldstrike stock in the north (Fig. 2). A second purpose of the regional samples was to examine the cooling histories of the Goldstrike and Little Boulder stocks across the Post fault (a major fluid conduit for mineralizing fluids). The Little Boulder stock is considered an offset portion of the Goldstrike stock (D. Park, pers. commun., 2000). For this purpose, multiple samples were collected from each stock at different elevations.

Thirty-five samples were collected for analysis, of which only 20 (17 regional and three deposit samples; Fig. 2) produced apatite grains of sufficient quantity and size to be used for fission-track analysis (see below). Five of these samples were also analyzed by $^{40}\text{Ar}/^{39}\text{Ar}$ techniques and three were analyzed using (U-Th)/He methods. Samples from the Carlin East deposit range from carbonaceous, decarbonated silty limestone with local kaolinite and orpiment, to oxidized and silicified silty limestone, to argillized and sericitized lamprophyre dikes. Detailed sample descriptions are available in Chakurian (2001) and are summarized in the Appendix. The regional samples were collected from a variety of units ranging from unaltered silty limestone or quartzite, to altered and weathered granodiorite, to unaltered quartz monzonite porphyry. Igneous rock samples represent intrusions that are thought to be no younger than the Richmond stock (106 Ma; Evans, 1980); that is, no samples were collected from known or suspected dikes of Tertiary age. Except for samples TCCA 165, LBB-76C, and S2-111, the igneous rock samples are relatively unaltered.

Apatite types

Apatite grains are classified as either primary (magmatic or detrital; in existence when the rock formed) or secondary (presumably hydrothermal; formed after formation of the host rock). Primary magmatic and detrital apatite grains tend to exhibit a well-defined to rounded, hexagonal, prismatic crystal habit. Secondary apatite grains in this study generally exhibit a granular crystal habit, with the individual crystal domains within the grain exhibiting random crystallographic orientation relative to their neighboring domains.

Apatite grains also were classified according to their kinetics of fission-track annealing (the rate at which fission tracks are lost), inferred using the parameter "Dpar" (units in μm). Dpar is the fission-track etch pit diameter parallel to the

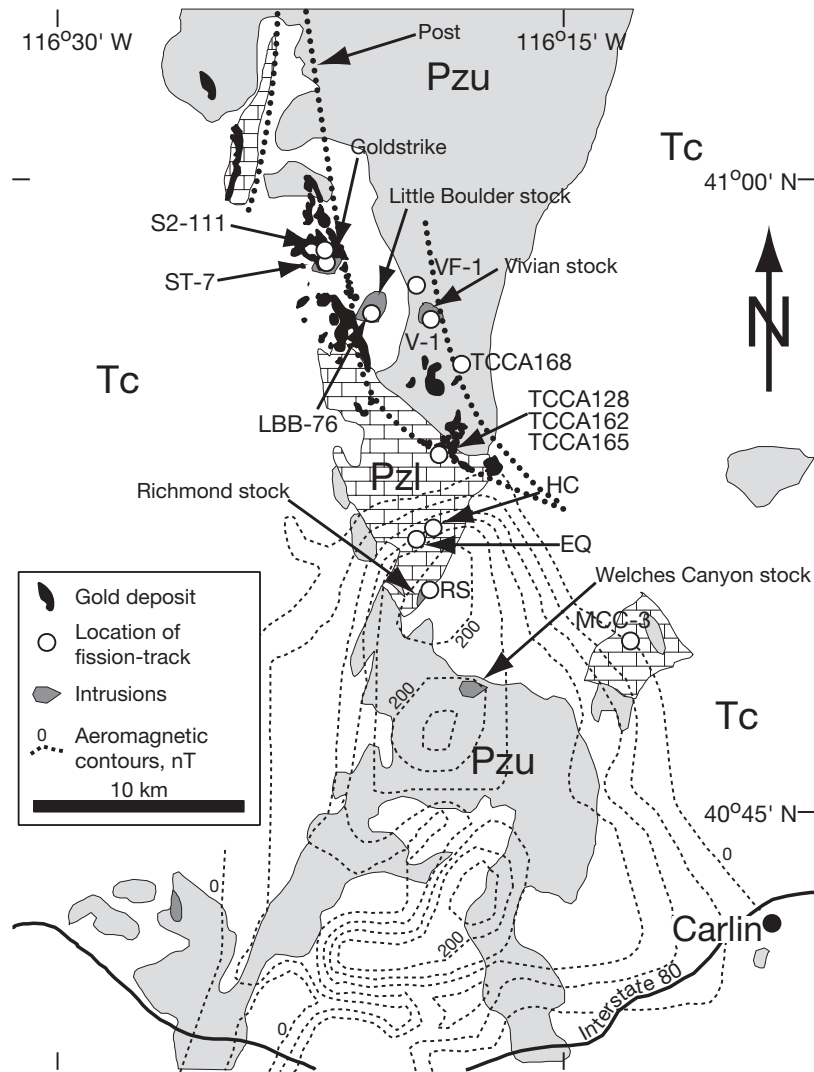


FIG. 2. Location of samples with apatite fission-track ages taken along the Carlin trend. Neutral to positive aeromagnetic contours are plotted showing the inferred extent of the igneous bodies along the Carlin trend. Simplified from Evans (1980) and Stewart and Carlson (1978) with major structures (heavy dotted lines) and deposit footprints from Teal and Jackson (1997). Aeromagnetic contours are modified from Ressel et al. (2001) and represent positive contours in nanoteslas above an arbitrary background. Numbers represent samples for which ages are reported in Table 1. Abbreviations: Pzl = Paleozoic lower plate rocks, Pzu = Paleozoic upper plate rocks, Tc = Tertiary Carlin Formation and other late Tertiary units.

crystallographic c-axis at the polished, etched, and analyzed apatite surface (Crowley et al., 1991; Naeser, 1992; Donelick, 1993; Burtner et al., 1994; Grønlie et al., 1994). Dpar shows general but imperfect correlations with apatite fission-track annealing kinetics (Carlson et al., 1999; Ketcham et al., 1999) and with mineral composition (Burtner et al., 1994), with small Dpar ($<2.00 \mu\text{m}$) grains typical of fast-annealing Ca-F-apatite and large Dpar grains typical of slow- to fast-annealing Ca \pm Fe, Mn, rare earth elements, (others?)-F \pm Cl \pm OH apatite. Dpar is at least as reliable as Cl or OH content as an indicator of apatite fission-track annealing kinetics (Carlson et al., 1999; R.A. Donelick, unpub. data).

Fission-track sample preparation and analysis

All fission-track sample preparation and analyses were performed by R.A. Donelick at Donelick Analytical, Inc., facilities

in Viola, Idaho. Samples were crushed using a jaw crusher and sieved through 300- μm nylon mesh. The $<300\text{-}\mu\text{m}$ fraction was washed with tap water, dried at room temperature, and separated into various density and magnetic fractions using lithium metatungstate (density = 3.0 g/cm^3), diiodomethane (density = 3.3 g/cm^3), and a Frantz Isodynamic magnetic separator. Final purification of the apatite fraction was performed by panning in a small petri dish in ethanol. Apatite grains for each sample were mounted in epoxide resin cured at 90°C for 1 h and polished using $3.0\text{-}\mu\text{m}$ Al_2O_3 and then $0.3\text{-}\mu\text{m}$ Al_2O_3 slurries on a polishing wheel to expose internal crystal surfaces. Two grain mounts were prepared for each sample in this fashion.

Fission-track ages of the apatite grains were determined using the external detector method (Naeser and Crowley, 1989) and all counting was performed using an optical microscope

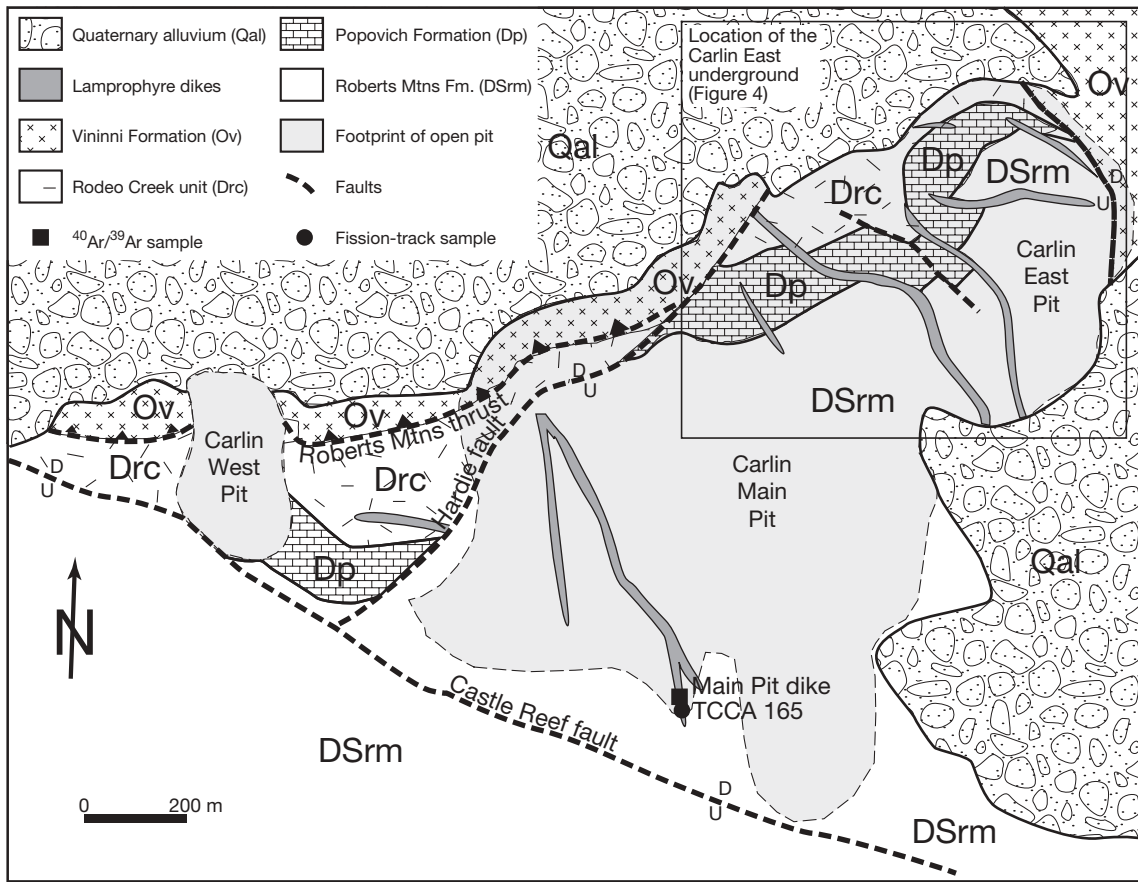


FIG. 3. Generalized geologic map of the surface of the Carlin mine, showing location of samples from the pit and the location of Figure 4.

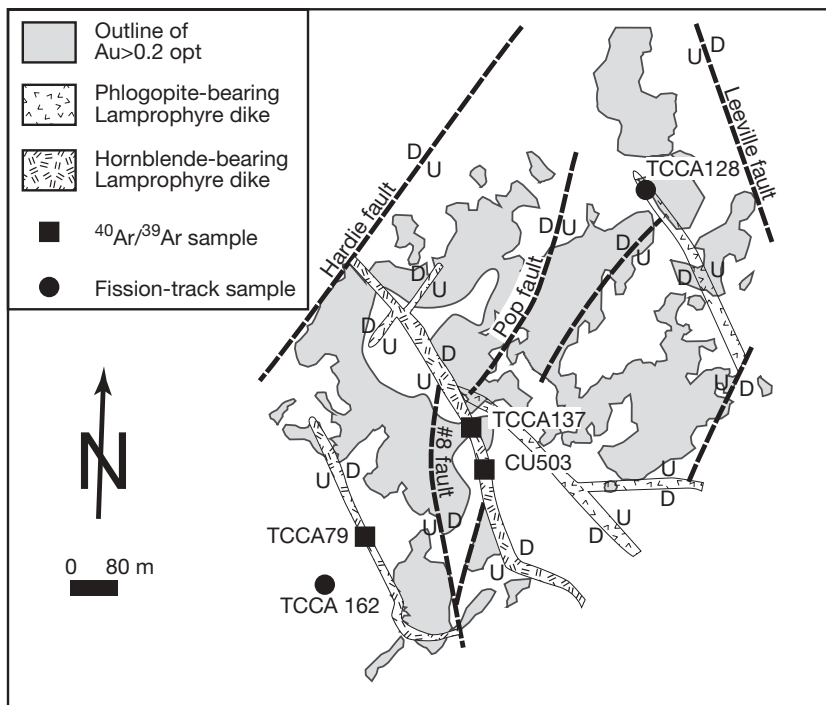


FIG. 4. Simplified geologic map of the Carlin East underground mine showing sample locations.

and a combination of reflected and unpolarized transmitted light at a magnification of $1,562.5\times$ ($100\times$ dry objective, $1.25\times$ projection tube, and $12.5\times$ oculars). For each sample, one grain mount was etched in $5.5N$ HNO_3 for 20.0 ± 0.5 sec at $21^\circ \pm 1^\circ C$ to reveal spontaneous (natural) fission tracks in the apatite grains for optical viewing, and then this grain mount was covered by a thin sheet of low-uranium muscovite mica. For purposes of standardization, a similar sheet of muscovite was placed in direct contact with a small chip of CN-1 ^{235}U -doped glass. These apatite samples and glass standards were irradiated together for one hour in position D-9 in the nuclear reactor at Washington State University (1 MW power level) yielding a nominal thermal-neutron fluence of about 10^{16} neutrons/cm². After irradiation, the short-lived radionuclides in the samples were allowed to decay to background levels before further analyses were performed. The mica sheets, once removed from the apatite samples and glass standards, were etched for 12 min in 48 percent HF at $24^\circ C$, revealing the induced (formed by irradiation in the reactor) fission tracks for optical viewing. Fission-track ages were calculated using a zeta calibration factor of 113.8 ± 2.9 Ma determined using Fish Canyon Tuff and Durango apatite-age standards (Hurford and Green, 1983).

For each sample, the second polished grain mount was irradiated with ^{252}Cf -derived fission fragments (Donelick and Miller, 1991) in a nominal vacuum and then etched in $5.5N$ HNO_3 for $20.0 (\pm 0.5)$ sec at $21^\circ (\pm 1^\circ) C$ to reveal the spontaneous and ^{252}Cf -derived fission tracks in the apatite grains for optical viewing. Length measurements were performed only on horizontal, confined, spontaneous fission tracks with well-defined ends lying in planes parallel to the crystallographic c-axis (all ^{252}Cf -derived fission tracks are incident upon the etched apatite surface and are therefore not confined within the grain). Measurements were performed using an optical microscope and a combination of reflected and unpolarized transmitted light at a magnification of $1,562.5\times$. Full details on the methods used are summarized in Donelick (1991).

Parameter Dpar, calculated as the arithmetic mean of between 1 and 4 individual Dpar values for a grain, was determined for each apatite grain that yielded either fission-track-age data or track length data. Full details of the methods used are summarized in Burtner et al. (1994).

$^{40}Ar/^{39}Ar$ sample preparation and analysis

$^{40}Ar/^{39}Ar$ analyses of Carlin East rock samples were conducted at Ohio State University. Details of the procedures and analytical results are described in Chakurian (2001) including information on the K, Ca, and Cl contents of the samples and all ages for the total gas (or integrated) and individual fractions. An overall systematic uncertainty of ± 1 percent is assigned to J values to reflect uncertainty in the absolute age of the monitor which is not included in the quoted age uncertainties.

(U-Th)/He sample preparation and analysis

The (U-Th)/He sample preparation and analyses were performed at Washington State University (Reiners, 2002, and references therein). (U-Th)/He dating is based on measurement of the amount of U + Th and their decay product, He,

in a manner similar to that done for K-Ar dating. This technique allows geochronological examination of apatite at a lower closure temperature ($68^\circ \pm 5^\circ C$) than that for the apatite fission-track technique (Wolf et al., 1996; Farley, 2000). This lower closure temperature allows (U-Th)/He dating to record the presence and/or timing of relatively low-temperature thermal events or events that occur over short durations.

Apatite grains selected for (U-Th)/He analyses were hand picked using transmitted polarized light at $400\times$ magnification; whole, euhedral, inclusion-free grains were preferred. After measuring the length and width of selected apatite grains, the grains were transferred to stainless steel capsules and heated sequentially in a resistance furnace to $925^\circ C$ for 20 min; reextracts were then performed to ensure quantitative He extraction. Liberated gases were spiked with 3He and processed through a sequence of getters and charcoal trap cycling between 16 K and 37 K. 4He was measured on a quadrupole mass spectrometer by isotope dilution. Following this, grains were recovered, transferred to teflon vials, spiked with ^{230}Th and ^{235}U , and dissolved in nitric acid. U and Th isotope ratios of the resulting solution were measured on a Finnigan Element sector ICP-MS. Analytical uncertainties for He and U/Th measurements are ~ 1 to 2 percent. Estimated reproducibility of these apatite (U-Th)/He ages is estimated to be about 6 percent (2σ) based on reproducibility of Durango apatite and other standards.

Analytical Results

Fission-track data

Figure 5 shows apatite fission-track data for two representative samples, RS and S2-111, plotted against parameter Dpar. The apatite fission-track data measured in this study were interpreted using AFTSolve software (version 1.3.0; Ketcham et al., 2000) based on the experimental data of Carlson et al. (1999) and the models of Donelick et al. (1999) and Ketcham et al. (1999). AFTSolve permits simultaneous calculation of model fission-track ages (only pooled fission-track ages were considered in this study) and track length distributions for comparison to measured data for distinct apatite grain populations exhibiting different Dpar values and, in most cases, different fission-track annealing kinetics. Results of the AFTSolve modeling are presented in Table 1. Each line in Table 1 represents a single population of apatite grains and presents both the measured data for each population (mean track lengths and fission-track ages) and the model results (model equivalents to the measured values). Also presented in Table 1 is the model-dependent, calculated value of the age of the oldest fission track present in each apatite grain population modeled.

With the exception of one sample (TCCA 162 from the Carlin East deposit), all samples yield measured fission-track ages greater than or equal to approximately 28 Ma. Six samples yield measured fission-track ages between approximately 41 and 28 Ma (samples in italics in Table 1), indicating that these samples cooled from temperatures of 110° to $135^\circ C$ (the value depending largely on Dpar) since approximately 40 Ma. Samples TCCA 165 and S2-111 (Dpar = $1.87 \mu m$ only), collected from the Carlin East and Betze-Post deposits, respectively, yield measured fission-track ages of 40.9 ± 4.0 Ma

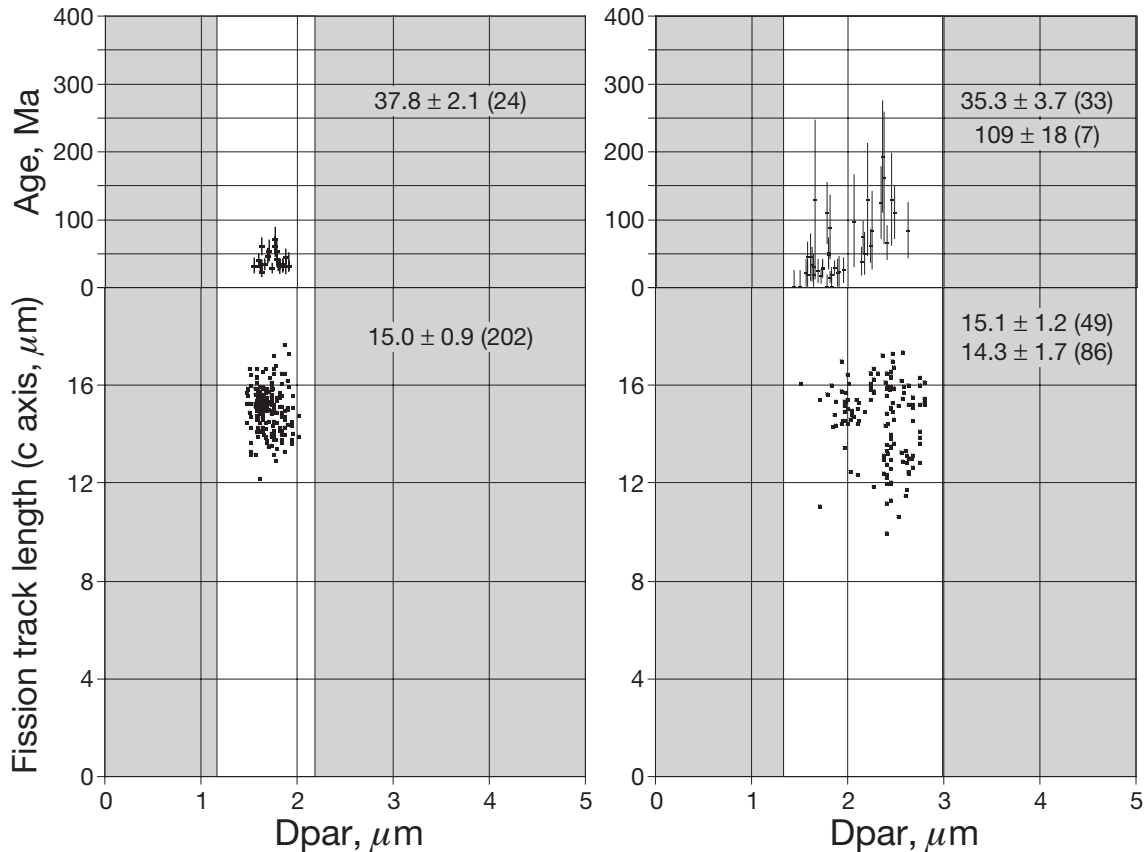


FIG. 5. Apatite fission-track ages (upper data groupings) and lengths (lower data groupings; y-axis in μm of c-axis-parallel equivalent lengths; see text) plotted against parameter Dpar for sample RS (left plot) and sample S2-111 (right plot). Dpar is the diameter parallel to the crystallographic c-axis of fission tracks and other etch pits on the polished and etched apatite grain surface.

and 35.5 ± 3.7 Ma, respectively. Similar ages are also observed for four samples (HC, EQ, RS, and MCC-3) from south of the Carlin East deposit. Combined, these six ages yield a weighted mean measured fission-track age of 37.3 ± 1.5 Ma and a weighted mean age of oldest fission track of 41.6 ± 1.6 Ma.

With the exception of sample S2-111 from the Betze-Post deposit (Dpar = $1.87 \mu\text{m}$ only), all samples north of the Carlin East deposit, including samples from the Little Boulder and Goldstrike stocks, yield measured apatite fission-track ages greater than approximately 56 Ma and oldest fission-track ages greater than approximately 67 Ma (Table 1). A large clustering of the measured apatite fission-track ages occurs in the range of 79 to 56 Ma (eight apatite grain populations) and the corresponding oldest fission-track ages are in the range of 84 to 67 Ma. For each of these samples, the estimated temperature at 40 Ma (assuming monotonic cooling from the age of the oldest fission track preserved to present-day) is presented in Table 1. A trend in these estimated temperatures is apparent in terms of sample location relative to the Post fault. Samples VF-1, V-1, TCCA 168, and those from the LBB-76 drill hole in the Little Boulder stock (drilled at a $\sim 60^\circ$ inclination to the south-southeast; Fig. 6) occur on the east side of the Post fault. As a whole, these samples give lower estimated temperatures at 40 Ma than any of the

samples from the Betze-Post deposit and from the ST-7 drill hole in the Goldstrike stock (drilled vertically; Fig. 6) to the west of the Post fault. Comparing only the samples from the upper 430 m of the two drill holes, it appears that the LBB-76 drill hole samples were approximately 35°C cooler than their counterparts in the ST-7 drill hole.

Finally, sample TCCA 162 from the Roberts Mountains Formation yields the youngest measured apatite fission-track age of any sample studied here, 18.6 ± 4.5 Ma, and the youngest age of the oldest fission track preserved, 20.3 ± 4.9 Ma.

$^{40}\text{Ar}/^{39}\text{Ar}$ ages

$^{40}\text{Ar}/^{39}\text{Ar}$ was selected as a method to investigate the age of gold mineralization at the Carlin East deposit because of the presence of numerous, strongly altered lamprophyre dikes in and adjacent to the deposit in which the major K-bearing phase is sericite (fine-grained muscovite). In addition, previous investigators have relied heavily on K-Ar and $^{40}\text{Ar}/^{39}\text{Ar}$ data to interpret the age of mineralization in Carlin-type deposits (e.g., Arehart et al., 1993b; Hofstra et al., 1999). Temperatures during gold mineralization ($\sim 225^\circ\text{C}$; Arehart, 1996) are unlikely to have exceeded the sericite closure temperature for Ar retention of 270° to 350°C (Purdy and Jäger, 1976; Jäger, 1979; Lister and Baldwin, 1996); however, during gold

TABLE 1. Calculated Fission-Track Ages for Individual Apatite Grain Populations

Sample no.	Primary (P) or secondary (S) apatite	Dpar (μm)	Initial mean track length (μm)	Grain ages (Ma)	Track lengths (μm)	K-S test	Age GOF	Model mean track length (μm)	Measured mean track length (μm)	Model fission-track age (Ma)	Measured fission-track age (Ma)	Age of oldest fission track (Ma)	Temperature at ~40 Ma before present ($^{\circ}\text{C}$)
Carlin East deposit													
TCCA 128	P,S	2.13	16.54	37	200	0.73	0.93	14.7 \pm 1.5	14.7 \pm 1.6	56.4	56.1 \pm 3.3	66.5 \pm 3.9	21 $^{\circ}$ –105 $^{\circ}$ C; best = 59 $^{\circ}$ C
TCCA 162	S	1.71	16.45	12	19	1.00	1.00	14.9 \pm 1.3	14.7 \pm 1.6	18.6	18.6 \pm 4.5	20.3 \pm 4.9	\geq ~125 $^{\circ}$ C
TCCA 165		2.04	16.52	16	63	0.90	0.98	14.9 \pm 1.0	14.9 \pm 1.3	40.8	40.9 \pm 4.0	43.3 \pm 4.2	\geq ~130 $^{\circ}$ C
Samples south of Carlin East deposit													
HC	S	1.73	16.45	5	14	0.95	0.97	14.8 \pm 1.0	14.3 \pm 1.6	36.9	36.7 \pm 5.7	39.5 \pm 6.1	\geq ~130 $^{\circ}$ C
EQ	S	1.63	16.43	6	11	1.00	1.00	14.5 \pm 1.1	14.5 \pm 1.2	27.7	27.7 \pm 6.8	31.7 \pm 7.8	\geq ~110 $^{\circ}$ C
RS		1.75	16.46	24	202	0.70	0.96	14.9 \pm 1.1	15.0 \pm 0.9	37.7	37.8 \pm 2.1	41.2 \pm 2.3	\geq ~130 $^{\circ}$ C
MCC-3		2.14	16.54	10	17	1.00	1.00	15.2 \pm 0.9	15.2 \pm 1.0	37.9	37.9 \pm 4.1	39.2 \pm 4.2	\geq ~135 $^{\circ}$ C
Samples north of Carlin East deposit													
VF-1	P,S	1.91	16.49	24	202	0.30	0.88	14.7 \pm 0.9	14.7 \pm 1.0	78.3	78.8 \pm 3.1	84.4 \pm 3.3	41 $^{\circ}$ –54 $^{\circ}$ C; best = 49 $^{\circ}$ C
V-1	P,S	2.24	16.56	12	102	0.85	0.88	14.8 \pm 1.4	14.8 \pm 1.3	92.5	91.6 \pm 6.1	110 \pm 7	15 $^{\circ}$ –62 $^{\circ}$ C; best = 29 $^{\circ}$ C
TCCA 168		2.32	16.58	14	136	0.89	0.98	14.6 \pm 1.6	14.6 \pm 1.4	112	113 \pm 8	140 \pm 10	15 $^{\circ}$ –54 $^{\circ}$ C; best = 24 $^{\circ}$ C
Little Boulder stock													
LBB-76A		2.58	16.63	37	200	0.45	0.57	14.7 \pm 1.6	14.6 \pm 1.5	125	129 \pm 7	149 \pm 8	15 $^{\circ}$ –34 $^{\circ}$ C; best = 17 $^{\circ}$ C
LBB-76B		2.35	16.58	25	202	0.27	0.31	14.5 \pm 1.7	14.5 \pm 1.8	126	119 \pm 7	155 \pm 9	15 $^{\circ}$ –27 $^{\circ}$ C; best = 22 $^{\circ}$ C
LBB-76C		1.67	16.44	18	92	0.14	0.13	15.1 \pm 1.2	15.2 \pm 0.9	72.1	62.6 \pm 6.3	79.2 \pm 8.0	15 $^{\circ}$ –28 $^{\circ}$ C; best = 15 $^{\circ}$ C
LBB-76D		2.40	16.59	6	108	0.79	0.13	14.8 \pm 1.5	14.9 \pm 1.4	90.6	114 \pm 16	106 \pm 15	
LBB-76D		1.93	16.50	33	200	0.39	0.56	15.0 \pm 0.9	15.0 \pm 0.9	66.7	69.7 \pm 5.2	70.1 \pm 5.2	28 $^{\circ}$ –60 $^{\circ}$ C; best = 42 $^{\circ}$ C
Post-Betze deposit–Goldstrike Stock													
S2-III		1.87	16.48	33	49	0.19	0.13	14.8 \pm 1.5	15.1 \pm 1.2	41.1	35.5 \pm 3.7	52.2 \pm 5.6	90 $^{\circ}$ –106 $^{\circ}$ C; best = 104 $^{\circ}$ C
S2-III		2.56	16.62	7	86	0.11	0.08	13.8 \pm 1.8	14.3 \pm 1.7	77.2	109 \pm 18	115 \pm 19	
Goldstrike stock													
ST-7A		2.11	16.53	26	197	0.23	0.88	14.2 \pm 1.7	14.3 \pm 1.5	69.5	70.4 \pm 5.4	101 \pm 8	45 $^{\circ}$ –91 $^{\circ}$ C; best = 64 $^{\circ}$ C
ST-7B		2.00	16.51	40	139	0.73	0.70	14.5 \pm 1.5	14.5 \pm 1.4	59.8	58.0 \pm 4.5	76.2 \pm 5.9	36 $^{\circ}$ –100 $^{\circ}$ C; best = 56 $^{\circ}$ C
ST-7C		2.01	16.51	38	200	0.23	0.31	14.4 \pm 1.5	14.4 \pm 1.4	54.4	58.1 \pm 3.6	69.9 \pm 4.3	52 $^{\circ}$ –91 $^{\circ}$ C; best = 60 $^{\circ}$ C
ST-7D		1.91	16.49	14	92	0.23	0.29	14.6 \pm 1.2	14.4 \pm 1.4	65.9	58.3 \pm 7.2	76.7 \pm 9.5	37 $^{\circ}$ –83 $^{\circ}$ C; best = 55 $^{\circ}$ C
ST-7D		2.49	16.61	19	44	0.23	0.23	14.3 \pm 1.7	14.6 \pm 1.5	85.0	94.6 \pm 7.9	120 \pm 10	
ST-7E		2.22	16.56	39	196	0.78	0.86	14.0 \pm 1.5	14.0 \pm 1.4	55.7	56.3 \pm 3.5	74.0 \pm 4.6	72 $^{\circ}$ –103 $^{\circ}$ C; best = 93 $^{\circ}$ C

Notes: All apatite grains studied are primary magmatic or detrital grains unless otherwise noted; data in italics constrain the timing of mineralization in the Carlin East deposit (see text); all errors are one standard deviation; model results were calculated using AFTSolve (Version 1.3.0; Ketchum et al., 2000) assuming a present-day mean annual surface temperature of 15 $^{\circ}$ C and Monte Carlo simulations of 30,000 iterations with 33 time-temperature nodal points, monotonic cooling to present-day, and no constraints on cooling rates between nodal points; all fission-track lengths are c-axis projected equivalent lengths (Donelick et al., 1999); Dpar is the diameter parallel to the crystallographic c-axis of fission-track and other etch pits on the polished and etched apatite grain surface; K-S test (Kolmogorov-Smirnov statistic; Press et al., 1992) is the probability of a worse fit between the measured and model track length distributions; age GOF is the probability of a worse fit between the measured and modeled fission track ages; error on the age of oldest fission track = (age of oldest fission track/measured fission-track age) \times error on the measured fission-track age; temperature at ~40 Ma before present is the range of temperatures at 40 Ma before present for all Monte Carlo-generated thermal histories for which both K-S Test and Age GOF values are \geq 0.05; the best temperature is the temperature for the Monte Carlo-generated thermal history for which K-S Test + Age GOF is greatest

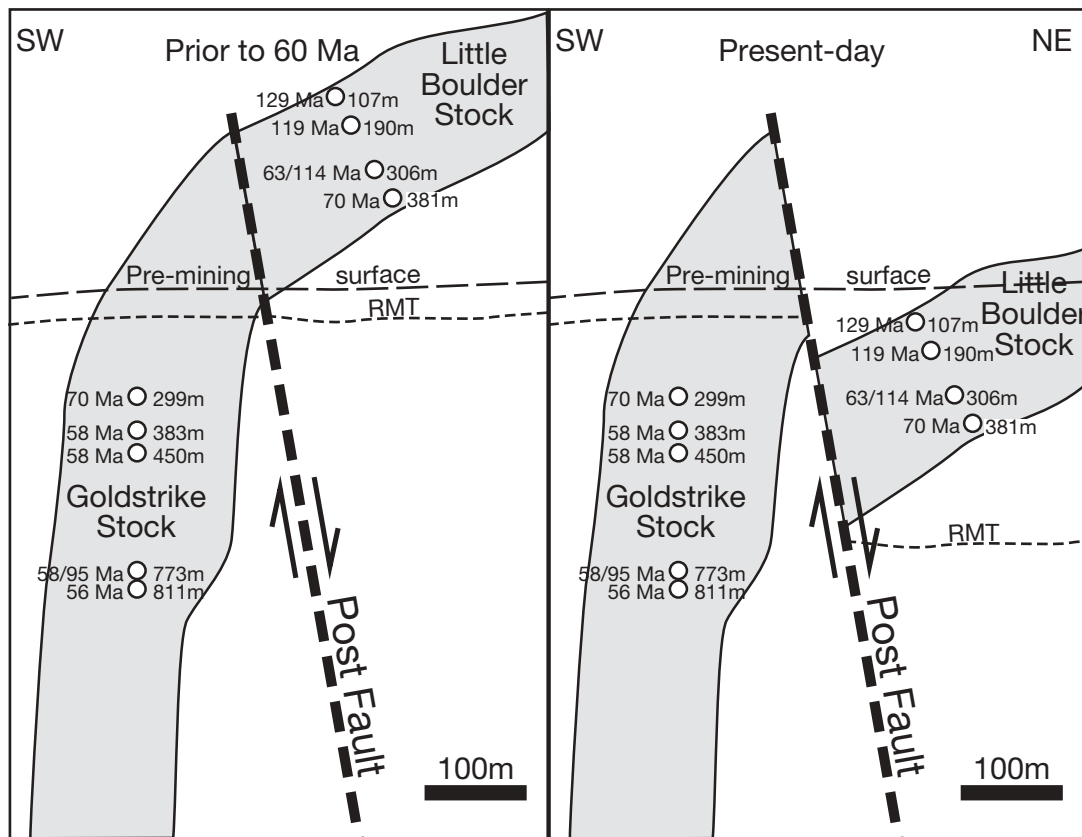


FIG. 6. Schematic cross section across the Post fault showing the offset at ~60 Ma as inferred from fission-track data. Not shown is subsequent strike-slip movement on the Post fault. Ages of fission-track populations are shown to the left of samples and depth from surface is shown to the right. RMT = approximate location of the Roberts Mountains thrust.

mineralization at the Carlin mine, growth of new minerals such as sericite rims and possible Ostwald ripening of existing sericite grains are likely to have occurred, based on the geochemical data of Bakken (1990). Thus, the sericite samples from the Carlin East deposit may have mixed ages that can be partially resolved by step-heating techniques (see discussion by Arehart et al., 2003).

All samples, regardless of the gold content and location, yielded similar patterns, with the low-temperature steps yielding a younger age and a gradual transition to older ages in the higher temperature steps (Fig. 7 and Table 2); however, the minimum and maximum ages for individual samples varied between 100 to 50 Ma and 152 to 100 Ma, respectively.

The sample K/Ca ratios are not well correlated with age, but the indicated Ca content is very low in all samples. In contrast, K/Cl ratios are generally correlated, increasing with increasing apparent age, suggesting a difference in the chemical composition of sericite between the low-temperature and high-temperature steps. This difference is not of sufficient magnitude and the transition is not sharp enough to suggest the presence of a nonsericite phase. At the very highest steps, which constitute <5 percent of the released Ar, a significant jump in K/Cl and age is observed. It is likely that this feature is merely an artifact of ^{39}Ar recoil redistribution, probably from sericite into quartz. Because the rocks are very fine grained, significant ^{39}Ar will be implanted into quartz. This Ar

will be released when quartz degasses at high temperature and this unsupported ^{39}Ar will produce ages that are variably low. This is similar to the recoil artifacts described for low K crystals in glass by Foland et al. (1993).

The $^{40}\text{Ar}/^{39}\text{Ar}$ spectra and ages can be interpreted as mixed ages that reflect mainly two events, although additional events are possible. The lower temperature fractions appear

TABLE 2. Summary of $^{40}\text{Ar}/^{39}\text{Ar}$ Analytical Results for Carlin East Whole-Rock Samples

Sample	Run no.	K ¹ (wt %)	Integrated age ² (Ma)
Carlin, main dike	63I9	1.1	65.5
	63I12	0.4	65.0
Carlin, east dike	63I14	2.4	132.5
	63I16	2.4	133.1
TCCA 79	64A29	1.6	109.1
TCCA 137	64A32	1.1	127.5
CU 503	64A36	1.7	95.2

¹ wt % of K in the bulk mineral separate determined by the total quantity of ^{39}Ar produced during neutron irradiation and released during incremental heating analysis

² Integrated (or total gas) age in Ma derived from the summation of all fractions of the incremental heating analysis

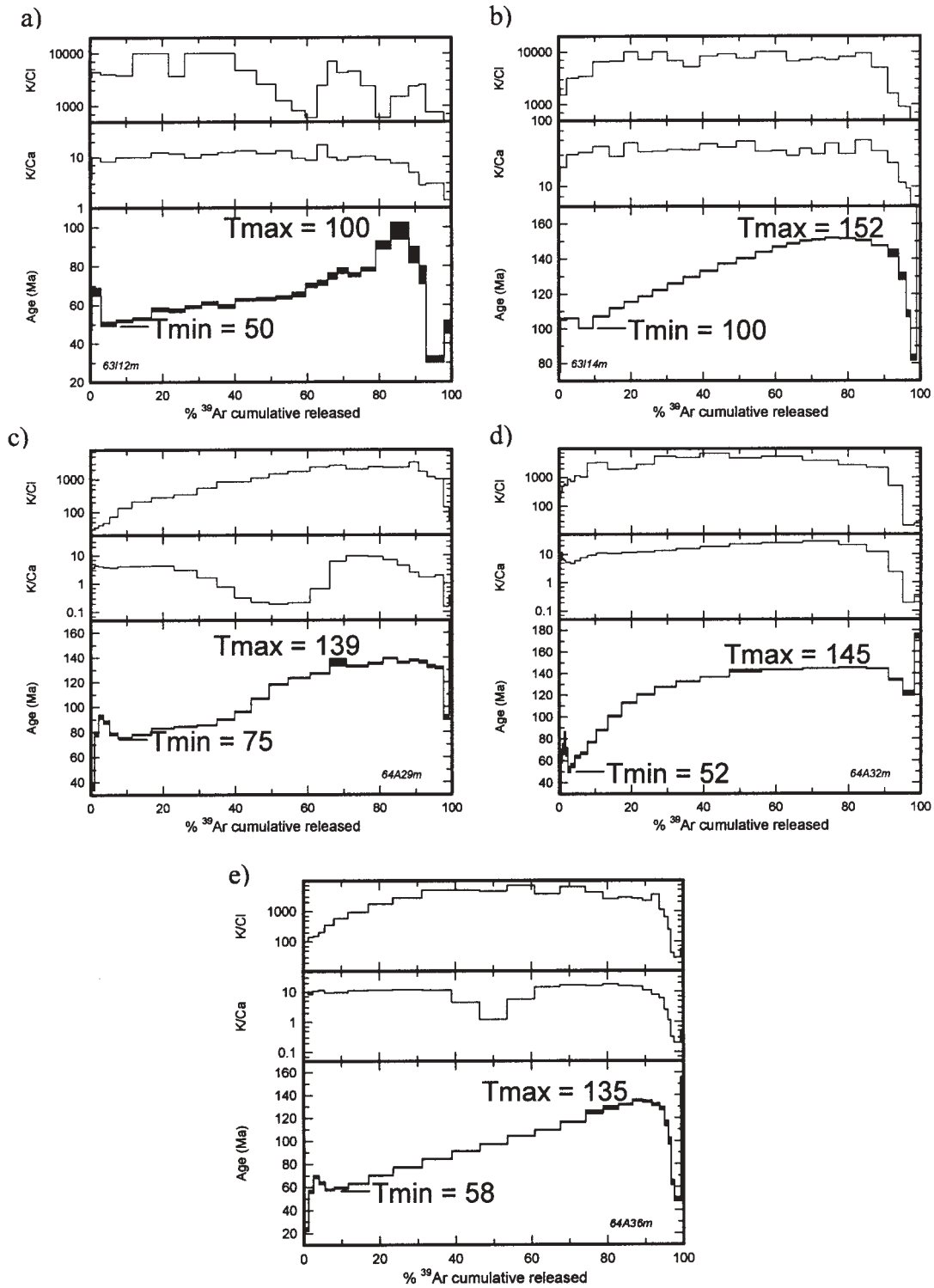


FIG. 7. Ar step-heating results for samples from the Carlin East deposit. The lowest temperature step (T_{min}) provides a maximum age for a thermal event (in some cases, the first or last few steps are ignored because they are considered noise rather than valid minima or maxima). The highest temperature step (T_{max}) suggests a minimum age for an older event. a. ⁴⁰Ar/³⁹Ar spectrum of the Main Pit dike, sample TCCA 165. b. ⁴⁰Ar/³⁹Ar spectrum of the phlogopite-bearing East Pit dike, sample TCCA 163. c. ⁴⁰Ar/³⁹Ar spectrum of the S-A dike, sample TCCA 79. d. ⁴⁰Ar/³⁹Ar spectrum of the Midway dike, sample TCCA 137. e. ⁴⁰Ar/³⁹Ar spectrum of a high-grade gold sample of the Midway dike, sample CU 503.

to sample dominantly phases (sericite) formed or altered during hydrothermal activity in the Cenozoic. In counterpoint, the higher temperature fractions are interpreted as reflecting a Jurassic event; the K-bearing phases here are also sericite, which reflects alteration near the time of intrusion of the dikes. The similar spectra differ basically only in degree, which can be viewed as reflecting the degree of Cenozoic overprinting by the growth of new sericite from mineralizing solutions. Where overprinting is greatest, the minimum, maximum, and integrated ages are lower, as for the Main dike. Where overprinting is less, the minimum, maximum, and integrated ages are higher, as for the East dike. Correlated ages and K/Cl ratios (Table 2) support this mixing interpretation. In particular, the changing K/Cl probably reflects compositional changes from one generation of sericite to another. It would be unlikely that step heating would completely resolve the events because the multiple generations of sericite, despite the minor compositional differences, will break down somewhat together during the step-heating process.

Thus the spectra can be interpreted only to constrain the age of the igneous event(s) and associated alteration to be older than the age maxima (~152 Ma) and the age of gold mineralization to be younger than the age minima (~50 Ma). The age maxima that are found approach but do not reach the well-established 158 Ma age of the Goldstrike stock (Arehart et al., 1993b). The minimum ages approach the apparent age of Carlin-type gold mineralization (see Arehart et al., 2003).

(U-Th)/He ages

Splits of apatite grains from three samples (RS, TCCA 165, and ST-7D) that were prepared for apatite fission-track techniques were analyzed by (U-Th)/He techniques. All grains in the sample from the Richmond stock contained mineral inclusions; therefore, a reliable age for that sample was not obtained. TCCA 165 yielded an age of 31.0 ± 1.9 Ma and ST-7D yielded an age of 21.4 ± 1.3 Ma.

Interpretation

Regional trend of apatite fission-track ages

Several distinct clusters of measured apatite fission-track ages are observed (Table 1): (1) a cluster between 41 and 28 Ma, mostly samples south of the Carlin East deposit and including samples within the Carlin East and Betze-Post deposits, (2) a cluster between 79 and 56 Ma of samples north of the Carlin East deposit, (3) a cluster greater than 92 Ma of samples north of the Carlin East deposit, and (4) a single sample of 18.6 ± 4.5 Ma from within the Carlin East deposit.

Timing of Au mineralization

The presence of the 41 and 28 Ma age cluster in several samples from Carlin trend deposits, combined with the apparent regional record of this event to the south, suggests that there was a regional thermal event that took place at this time. The timing of this event is 37.3 ± 1.5 Ma, based on the weighted mean of the measured apatite fission-track ages for the six samples in this cluster, and 41.6 ± 1.6 Ma based on the weighted mean of the oldest fission-track ages in the respective apatite grain populations. The choice between these numbers is a matter of considerable debate, because the

means of calculating the age of the oldest fission track is not universally accepted (C.W. Naeser, verbal commun., 2002). Supporting evidence for these estimates of the timing of mineralization includes magnetic and gravity anomalies which may be indicative of a relatively large buried intrusion to the south of the Carlin East deposit (Fig. 2). Both geophysical anomalies are roughly coincident with the 37 Ma Welches Canyon stock (Evans, 1980), with the 106 Ma Richmond stock (Evans, 1980), and with the Marys Mountain volcanic center. Because of the temporal overlap between the age of the Welches Canyon stock and the apatite ages, the stock is proposed as the source of the thermal event and the driving force for mineralization of the Carlin East and Betze-Post deposits, as proposed by Ressel et al. (2000a, b) and Henry and Ressel (2000a, b). The areal extent of the Welches Canyon pluton cannot be directly linked to the areal extent of the magnetic high, but given the areal extent of the thermal anomaly that appears contemporaneous with intrusion, we infer that the Welches Canyon stock underlies a significant portion of the magnetic and gravity highs.

Younger thermal events

The anomalous young apatite fission-track age for sample TCCA 162 from the Carlin East deposit, 18.6 ± 4.5 Ma, suggests the local occurrence of a thermal event younger than the regional event at ca. 38 Ma, described above. Such a young event may be associated with Miocene extension and volcanism since there are Miocene volcanic rocks on the west flank of the Tuscarora Range (Evans, 1980). The presence of secondary apatite in sample TCCA 162 (Table 1) suggests that there was a weak hydrothermal event at this time. Additional evidence for this event has been documented locally near the Betze-Post and Gold Quarry deposits (mineralized Carlin Formation having a maximum age of ca. 17 Ma: Fleck et al., 1998; E. Lauha, writ. commun., 2000). In addition, the age of this hydrothermal event is also consistent with the (U-Th)/He age of 21 Ma for sample ST-7D. Because none of the other apatite populations studied here yielded similar ages, the hydrothermal event was most likely either limited locally, short-lived, and/or relatively low temperature.

Exhumation-cooling on either side of the Post fault

Petrographic analysis and whole-rock and rare earth element chemical data for the Little Boulder and Goldstrike stocks suggest that the two are most likely parts of the same intrusive body (Fig. 6; Chakurian, 2001). The intrusive body is thought to be a large sill, with the Goldstrike stock, the thickest part and inferred roof of the intrusion, originally located to the southwest of and connected to the thinner, sill-like Little Boulder stock prior to displacement by the Post fault (D. Park, pers. commun., 2000). The Post fault normally offsets the Little Boulder stock from the Goldstrike stock, dropping the portion now known as the Little Boulder stock.

From Table 1, it appears that the samples from the Little Boulder stock (LBB-76 drill hole) were approximately 35°C cooler at 40 Ma relative to their counterparts in the ST-7 drill hole in the Goldstrike stock. Two causes for these different thermal histories are proposed. The first possibility is that exhumation and cooling of the western side of the Post fault, containing the Goldstrike stock, since 40 Ma has been greater

than that on the eastern side. The amount of differential exhumation and cooling in this case is unknown because the data presented here do not allow for reconstruction of temperature versus depth profiles in the Goldstrike and Little Boulder stocks at 40 Ma. The second possibility is that little differential exhumation and cooling has occurred across the Post fault since 40 Ma. In this case, the Goldstrike and Little Boulder stocks were in essentially their current relative positions at 40 Ma and the Goldstrike stock was simply heated more during the mineralizing event relative to the Little Boulder stock. Additional data might provide constraints to choose between these two cases.

Apatite fission-track ages vs. ⁴⁰Ar/³⁹Ar ages in the Carlin trend

The Main Pit dike at the Carlin East deposit was analyzed by both ⁴⁰Ar/³⁹Ar and apatite fission-track techniques (sample TCCA 165). The two dating techniques produced different ages. The youngest age step of the ⁴⁰Ar/³⁹Ar age spectrum of the Main Pit dike is ~50 Ma. The apatite fission-track age of the Main Pit dike is 41 Ma. The difference in ages between the ⁴⁰Ar/³⁹Ar date and the apatite fission-track date of the Main Pit dike can be interpreted in two ways. Either some or all of the sericite was present prior to gold mineralization and was not fully reset at the time of mineralization or some (but not all) sericite was generated during hydrothermal alteration of the dike at ~41 Ma, and this sericite was not separable from prehydrothermal sericite, resulting in a mixed age. The first scenario is consistent with the fact that sericite has a much higher closure temperature than apatite. Therefore, as has been noted previously (Folger et al., 1996; Hofstra et al., 1999; Arehart et al., 2003), it is difficult to use sericite to date hydrothermal events in Carlin-type deposits.

Summary and Conclusions

Apatite fission-track analyses from one sample in the ore zone in the Carlin East deposit and the hydrothermally altered Goldstrike stock sample from the Betze-Post deposit suggest that the age of the Carlin East deposit is 40.9 ± 4.0 Ma and that of the Betze-Post deposit is 35.5 ± 3.7 Ma. These two ages are consistent with the data of Ressel et al. (2000a, b) and Arehart et al. (2003). Of the 20 apatite fission-track analyses presented here, six samples yield estimates for the timing of mineralization in the Carlin East and Betze-Post deposits. Combined, these samples yield reasonable estimates of 37.3 ± 1.5 Ma, based on the weighted mean of the measured apatite fission-track ages, and 41.6 ± 1.6 Ma, based on the weighted mean age of the oldest fission tracks preserved in the apatite grain populations.

The regional trend in the apatite fission-track age data suggests that emplacement of the Welches Canyon stock (dated at 37 Ma) was the heat source and driving force for gold mineralization of the Carlin East and Betze-Post deposits. One fission-track age and the two (U-Th)/He ages are clearly younger than that of the main Au event and probably reflect minor reheating of the rocks associated with Miocene igneous activity.

Present-day near-surface rocks in the Little Boulder stock were approximately 35°C cooler at 40 Ma compared to their counterparts in the Goldstrike stock. The significance of

these different thermal histories is unclear, but it may be due either to differential exhumation and cooling since 40 Ma or to variable greater heating of the Goldstrike stock during the mineralization event at ca. 40 Ma. Modeling of the thermal history of these two rock units clearly documents pre-gold movement on the Post fault.

Analysis of ages produced by apatite fission-track and ⁴⁰Ar/³⁹Ar techniques shows that the ⁴⁰Ar/³⁹Ar dates are older than the fission-track dates, apparently reflecting incomplete thermal resetting. The older sericite ⁴⁰Ar/³⁹Ar ages suggest that this system is not useful for determining the age of gold mineralization, at least using the technology employed in this study; however, step-heating data do provide some constraints on the timing of formation of sericite and, therefore, limits on the age of gold mineralization.

Acknowledgments

Field and analytical expenses were funded by National Science Foundation grant EAR9805384 to G.B.A. Additional support was provided by the Ralph J. Roberts Center for Research in Economic Geology and a Society of Economic Geologists Hugh E. McKinstry research grant to the senior author. We thank the geologists of the Newmont Mining Corporation and Barrick Gold for access to their properties along the Carlin trend and to their data throughout the research. Without their assistance, this paper would not have been possible. CN-1 glass was provided courtesy of Jan Schreurs, Corning Glass Works, Corning, New York. We are grateful to Ken Foland for his discussions and assistance with ⁴⁰Ar/³⁹Ar dating of the samples from the Carlin East deposit. We thank Chuck Naeser, Steve Harlan, Dennis Arne, and Ken Hickey for insightful reviews of an earlier version of this manuscript.

REFERENCES

- Arehart, G.B., 1996, Characteristics and origin of sediment-hosted disseminated gold deposits: A review: *Ore Geology Reviews*, v. 11, p. 383–403.
- Arehart, G.B., Chryssoulis, S.L., and Kesler, S.E., 1993a, Gold and arsenic in iron sulfides from sediment-hosted disseminated gold deposits: Implications for depositional processes: *ECONOMIC GEOLOGY*, v. 88, p. 171–185.
- Arehart, G.B., Foland, K.A., Naeser, C.W., and Kesler, S.E., 1993b, ⁴⁰Ar/³⁹Ar, K/Ar and fission B track geochronology of sediment-hosted disseminated gold deposits at Post/Betze, Carlin trend, northeastern Nevada: *ECONOMIC GEOLOGY*, v. 88, p. 622–646.
- Arehart, G.B., Chakurian, A.M., Tretbar, D.R., Christensen, J.N., McInnes, B.A., and Donelick, R.A., 2003, Evaluation of radioisotope dating of Carlin-type deposits in the Great Basin, western North America, and implications for deposit genesis: *ECONOMIC GEOLOGY*, v. 98, p. 235–248.
- Bakken, B.M., 1990, Gold mineralization, wall-rock alteration, and the geochemical evolution of the hydrothermal system in the Main orebody, Carlin mine: Unpublished Ph.D. dissertation, Stanford University, 236 p.
- Burtner, R.L., Nigrini, A., and Donelick, R.A., 1994, Thermochronology of Lower Cretaceous source rocks in Idaho-Wyoming thrust belt: *American Association of Petroleum Geologists Bulletin*, v. 78, p. 1613–1636.
- Carlson, W.D., Donelick, R.A., and Ketcham, R.A., 1999, Variability of apatite fission-track annealing kinetics I: Experimental results: *American Mineralogist*, v. 84, p. 1213–1223.
- Chakurian, A.M., 2001, Age of mineralization at the Carlin East mine, Eureka County, Nevada: Unpublished M.Sc. thesis, Reno, University of Nevada, 186 p.
- Crowley, K.D., Cameron, M., and Schaefer, R.L., 1991, Experimental studies of annealing of etched fission tracks in fluorapatite: *Geochimica et Cosmochimica Acta*, v. 55, p. 1449–1465.
- Donelick, R.A., 1991, Crystallographic orientation dependence of mean etchable fission track length in apatite: An empirical model and experimental observations: *American Mineralogist*, v. 76, p. 83–91.

- 1993, A method of fission-track analysis utilizing bulk chemical etching of apatite: Patent 5,267,274, U.S.A.
- 1995, A method of fission-track analysis utilizing bulk chemical etching of apatite: Patent 658,800, Australia.
- Donelick, R.A., and Miller, D.S., 1991, Enhanced tint fission-track densities in low spontaneous track density apatites using ^{252}Cf -derived fission fragment tracks: A model and experimental observations: *Nuclear Tracks and Radiation Measurements*, v. 18, no. 3, p. 301–307.
- Donelick, R.A., Ketcham, R.A., and Carlson, W.D., 1999, Variability of apatite fission track annealing kinetics II: Crystallographic orientation effects: *American Mineralogist*, v. 84, p. 1224–1234.
- Evans, J.G., 1980, Geology of the Rodeo Creek NE and Welches Canyon quadrangles, Eureka County, Nevada: U.S. Geological Survey Bulletin 1473, 81 p.
- Farley, K.A., 2000, Helium diffusion from apatite: General behavior as illustrated by Durango fluorapatite: *Journal of Geophysical Research*, v. 105, p. 2903–2914.
- Fleck, R.J., Theodore, T.G., Sarna-Wojcicki, A.M., Meyer, C.E., 1998, Age and possible source of air-fall tuffs of the Miocene Carlin Formation, northern Nevada: U.S. Geological Survey, Open-File Report OF 98-0338-B, p. 176–192.
- Foland, K.A., Fleming, T.H., Heimann, A., and Elliot, D.H., 1993, Potassium-argon dating of fine-grained basalts with massive Ar loss, application of the $^{40}\text{Ar}/^{39}\text{Ar}$ technique to plagioclase and glass from the Kirkpatrick Basalt, Antarctica: *Chemical Geology*, v. 107, p. 173–190.
- Folger, H.W., Snee, L.W., Mehnert, H.H., Hofstra, A.H., and Dahl, A.R., 1996, Significance of K-Ar and $^{40}\text{Ar}/^{39}\text{Ar}$ dates from mica in Carlin-type gold deposits: Evidence from Jerritt Canyon district, Nevada, in Coyner, A.R., and Fahey, P.L., eds., *Geology and ore deposits of the American cordillera. Symposium proceedings: Reno, Geological Society of Nevada*, p. 17–30.
- Grønlie, A., Naeser, C.W., Naeser, N.D., Mitchell, J.G., Sturt, B.A., and Ineson, P.R., 1994, Fission-track and K-Ar dating of tectonic activity in a transect across the Møre-Trøndelag fault zone, central Norway: *Norsk Geologisk Tidsskrift*, v. 74, p. 24–34.
- Henry, C.D., and Ressel, M.W., 2000a, Interrelation of Eocene magmatism, extension, and Carlin-type gold deposits in northeastern Nevada, in Lagesson, D.R., Peters, S.G., and Lahren, M.M., eds., *Great Basin and Sierra Nevada: Boulder, Colorado, Geological Society of America Field Guide 2*, p. 165–187.
- 2000b, Eocene magmatism of northeastern Nevada: The smoking gun for Carlin-type gold deposits, in Cluer, J.K., Price, J.G., Struhsacker, E.M., Hardyman, R.F., and Morris, C.L., eds., *Geology and ore deposits 2000: The Great Basin and beyond: Reno, Geological Society of Nevada, Symposium proceedings*, p. 365–388.
- Hofstra, A.H., and Cline, J.S., 2000, Characteristics and models for Carlin-type gold deposits: *Reviews in Economic Geology*, v. 13, p. 163–220.
- Hofstra, A.H., Snee, L.W., Rye, R.O., Folger, H.W., Phinisey, J.D., Loranger, R.J., Dahl, A.R., Naeser, C.W., Stein, H.J., and Lewchuk, M., 1999, Age constraints on Jerritt Canyon and other Carlin-type gold deposits in the western United States. B. Relationship to mid-Tertiary extension and magmatism: *ECONOMIC GEOLOGY*, v. 94, p. 769–802.
- Hurford, A.J., and Green, P.F., 1983, The zeta age calibration of fission-track dating: *Chemical Geology*, v. 1, p. 285–317.
- Jäger, E., 1979, *Introduction to geochronology: Lectures in isotope geology*: Berlin, Springer-Verlag, p. 1–12.
- Ketcham, R.A., Donelick, R.A., and Carlson, W.D., 1999, Variability of apatite fission track annealing kinetics III: Extrapolation to geological time scales: *American Mineralogist*, v. 84, p. 1235–1255.
- Ketcham, R.A., Donelick, R.A., and Donelick, M.B., 2000, AFTSolve: A program for multikinetic modeling of apatite fission-track data: *Geological Materials Research*, v. 2, no. 1. (Published online: <http://gmr.minsocam.org/papers/v2/v2n1/v2n1abs.html>)
- Lister, G.S., and Baldwin, S.L., 1996, Modelling the effect of arbitrary P-T-t histories on argon diffusion in minerals using the MacArgon program for the Apple Macintosh: *Tectonophysics*, v. 253, p. 83–109.
- Naeser, N.D., 1992, Miocene cooling in the southwestern Powder River basin, Wyoming—preliminary evidence from apatite fission-track analysis: *U.S. Geological Survey Bulletin* 1917–O, 17 p.
- Naeser, C.W., and Crowley, K.D., 1989, Age equation and statistics of fission-track dating: Fission-track analysis: Geological Society of America Annual Meeting, St. Louis, Missouri, November 4–5, 1989, Theory and applications, Short course notes, Chapter 2, 18 p.
- Purdy, J.W., and Jäger, E., 1976, K-Ar ages on rock-forming minerals from the central Alps: *Institute of Geology and Mining University of Padova Memoir*, v. 30, 31 p.
- Radtke, A.S., 1985, Geology of the Carlin gold deposit, Nevada: *U.S. Geological Survey Professional Paper* 1267, 124 p.
- Reiners, P.W., 2002, (U-Th)/He chronometry experiences a renaissance: *EOS*, v. 83, no. 3, p. 21, 26–27.
- Ressel, M.W., Noble, D.C., Heizler, M.T., Volk, J.A., Lamb, J.B., Park, D.E., Conrad, J.E., and Mortensen, J.K., 2000a, Gold-mineralized Eocene dikes at Griffin and Meikle: Bearing on the age and origin of deposits of the Carlin trend, Nevada, in Cluer, J.K., Price, J.G., Struhsacker, E.M., Hardyman, R.F., and Morris, C.L., eds., *Geology and ore deposits 2000: The Great Basin and beyond: Reno, Geological Society of Nevada, Symposium proceedings*, p. 79–101.
- Ressel, M.W., Noble, D.C., Henry, C.D., and Trudel, W.S., 2000b, Dike-hosted ores of the Beast deposit and the importance of Eocene magmatism in gold mineralization of the Carlin trend, Nevada: *ECONOMIC GEOLOGY*, v. 95, p. 1417–1444.
- 2001, Dike-hosted ores of the Beast deposit and the importance of Eocene magmatism in gold mineralization of the Carlin trend, Nevada—a reply: *ECONOMIC GEOLOGY*, v. 96, p. 666–668.
- Stewart, J.H., and Carlson, J.L., 1978, Geologic map of Nevada: U.S. Geological Survey map, 1 sheet.
- Teal, L., and Jackson, M., 1997, Geologic overview of the Carlin trend gold deposits and descriptions of recent deep discoveries: *Society of Economic Geologists Guidebook Series*, v. 28, p. 3–37.
- Tretbar, D.R., Arehart, G.B., and Christensen, J.N., 2000, Dating gold deposition in a Carlin-type gold deposit using Rb/Sr methods on the mineral galkhaite: *Geology*, v. 28, p. 947–950.
- Wolf, R.A., Farley, K.A., and Silver, L.T., 1996, Helium diffusion and low temperature thermochronology of apatite: *Geochimica et Cosmochimica Acta*, v. 60, p. 4231–4240.

APPENDIX

Sample Data

Sample no.	Location					Rock unit	Description	Gold (ppm)
	UTM (N)	UTM (E)	Elevations (m)	Azimuth	Inclination			
CU-503	4529611	557591	1,664	N/A	N/A	Lamprophyre dike	Midway dike; gray and white, sericitized	89.3
TCCA 79	4529350	557478	1,788	N/A	N/A	Lamprophyre dike	8-A dike; green and white, sericitized, sulfide, kaolinite	10.6
TCCA 128	4529857	557837	1,789	N/A	N/A	Lamprophyre dike	No. 5 dike; weakly altered phlogopite-bearing Lamprophyre	0.04
TCCA 137	4529650	557546	1,680	N/A	N/A	Lamprophyre dike	Midway dike; white, sericitized, sulfide stringers	3.95
TCCA 162	4529305	557423	1,792	N/A	n/a	RM Formation	Orange-yellow, oxidized, decarbonatized, calcite veinlets	N/A
TCCA 163	4529396	557829	1,860	N/A	N/A	Lamprophyre dike	East Pit dike; brown and white, oxidized, sericitized	0.61
TCCA 165	4528753	557303	1,943	N/A	N/A	Lamprophyre dike	Main Pit dike; red, oxidized, relict phenocrysts	0.82
TCCA 168	4532752	558088	2,195	N/A	N/A	Ov-quartzite	Orange and brown, oxidized	N/A
LBB-76A 351'	4533446	555339	Drill	135	-60	Granodiorite	Little Boulder stock; oxidized	N/A
LBB-76B 623'	4533446	555339	Drill	135	-60	Granodiorite	Little Boulder stock; unaltered	N/A
LBB-76C 1005'	4533446	555339	Drill	135	-60	Granodiorite	Little Boulder stock; weak to moderate sericite	N/A
LBB-76D 1251'	4533446	555339	Drill	135	-60	Granodiorite	Little Boulder stock; unaltered	N/A
ST-7A 981'	4535602	552745	Drill	N/A	-90	Granodiorite	Goldstrike stock; unaltered	N/A
ST-7B 1255'	4535602	552745	Drill	N/A	-90	Granodiorite	Goldstrike stock; unaltered	N/A
ST-7C 1477'	4535602	552745	Drill	N/A	-90	Granodiorite	Goldstrike stock; unaltered	N/A
ST-7D 2535'	4535602	552745	Drill	N/A	-90	Granodiorite	Goldstrike stock; unaltered	N/A
ST-7E 2662'	4535602	552745	Drill	N/A	-90	Granodiorite	Goldstrike stock; weak to moderate chlorite	N/A
S2-111	10645	11850	1,404	N/A	N/A	Granodiorite	Goldstrike stock; intensely sericitized and moderately argillized	< 0.001
MCC #3	4517416	566695	Surface	N/A	N/A	RM Formation	Visibly unaltered	N/A
RS	4522204	558265	Surface	N/A	N/A	Qtz monz porphyry	Richmond stock; unaltered	N/A
V-1	4533209	556991	1,920	N/A	N/A	Granodiorite	Vivian stock; unaltered	N/A
VF-1	4533179	556915	1,920	N/A	N/A	Ov-quartzite	Orange and brown, oxidized	N/A
HC	4526959	558000	Surface	N/A	N/A	OShc	Brown to black, silicified silty limestone	N/A
EQ	4526469	557327	Surface	N/A	N/A	Oe	White, weak to moderately silicified quartzite	N/A

Abbreviations: Oe = Ordovician Eureka Quartzite, OShc = Ordovician to Silurian Hanson Creek Formation, Ov = Ordovician Vimini Formation, RM = Devonian to Silurian Roberts Mountains Formation